Cell Tissue Res (2001) 306:15–26
DOI 10.1007/s004410100425

REGULAR ARTICLE

L. Vitellaro-Zuccarello · A. Meroni · A. Amadeo
S. De Biasi

Chondroitin sulfate proteoglycans in the rat thalamus: expression during postnatal development and correlation with calcium-binding proteins in adults

Received: 29 January 2001 / Accepted: 11 May 2001 / Published online: 3 July 2001
© Springer-Verlag 2001

Abstract Postnatal expression of chondroitin sulfate proteoglycans was studied in the rat thalamus by immunocytochemistry and Western immunoblotting techniques with monoclonal antibodies that recognize carbohydrate epitopes (clones CS-56, 1-B-5, 2-B-6). The complex of the results shows that these antibodies recognize mostly nonoverlapping molecules whose expression is regulated during postnatal development. Chondroitin sulfate proteoglycans, recognized by antibody CS-56, and hyaluronan, identified by antibody 1-B-5 after hyaluronidase digestion, are abundant in the neuropil of most thalamic nuclei at the perinatal stage and progressively decrease during the second week of life, attaining levels barely detectable by immunocytochemistry at the end of the third week. In adult thalamus, chondroitin sulfate proteoglycans of high molecular mass, bearing glycosaminoglycans unsulfated in the linking region, and recognized by antibody 1-B-5 are confined to perineuronal nets around neurons chiefly localized in thalamic reticular nucleus. The immunoreactvity for antibody 2-B-6, specific for chondroitin-4-sulfate, is low at the perinatal stage and is not detectable in adult thalamus. Double-immunolabeling has shown that, along the rostrocaudal extension of reticular nucleus, the most developed perineuronal nets are associated with a subset of neurons expressing calretinin, and not with parvalbumin-positive neurons, which represent the largest neuronal population of the nucleus. The distribution of perineuronal nets supports the presence, in thalamic reticular nucleus, of neuronal subpopulations with different morphological and physiological features.

Keywords Calretinin · Electron microscopy · Glycosaminoglycans · Parvalbumin · Thalamic reticular nucleus · Rat (Wistar)

L. Vitellaro-Zuccarello (✉) · A. Meroni · A. Amadeo · S. De Biasi
Sezione di Istologia e Anatomia Umana,
Dipartimento di Fisiologia e Biochimica generali, Via Celoria 26, 20133 Milan, Italy
e-mail: laura.vitellaro@unimi.it
Tel.: +39-2-70644303, Fax: +39-2-2362808

Introduction

Chondroitin sulfate proteoglycans (CSPGs) are the most abundant components of the extracellular matrix of the mammalian brain, encompassing at least 16 different types of molecules expressed at different developmental stages (Herndon and Lander 1990). Extensive experimental evidence indicates that these molecules, many of which belong to the lectican family, are involved in several developmental processes, regulating cell proliferation and differentiation and providing either inhibitory or permissive cues for axon outgrowth (for reviews, see Letournau et al. 1994; Margolis and Margolis 1994; Oohira et al. 1994; Yamaguchi 2000; Hartmann and Maurer 2001). Previous studies (Aquino et al. 1984; Flaccus et al. 1991; Rauch et al. 1991; Oohira et al. 1994; Maeda et al. 1995; Miller et al. 1995; Fernaud-Espinosa et al. 1996; Köppe et al. 1997; Hoffman-Kim et al. 1998) have shown that, during brain development, a diffuse and relatively abundant extracellular matrix contains complex combinations of CSPGs, whose chemical microheterogeneity is responsible for different biological effects.

Immunohistochemistry and lectin cytochemistry have revealed that, in the gray matter of adult brain, CSPGs are mainly concentrated in lattice-like envelopes, termed perineuronal nets, around cell bodies and proximal dendrites of distinct neuronal populations (for reviews, see Celio and Blümcke 1994; Celio et al. 1998; Matsui et al. 1999; Yamaguchi 2000). The presence of perineuronal nets does not identify classes of neurons homogeneous for the expression of other neurochemical markers but frequently corresponds to functional cortical areas and subcortical regions (Hockfield et al. 1983; Hendry et al. 1988; Sur et al. 1988; Crabtree and Kind 1993; Preuss et al. 1998; Gray et al. 1999; Pimenta et al. 2001).

The distribution of CSPGs in the rat thalamus has not been studied in detail, although previous studies have shown that, in adult brain, perineuronal nets are mainly concentrated in the thalamic reticular nucleus (Rt; Bertolotto et al. 1990, 1991, 1996; Seeger et al.

1994; Brückner et al. 1996). In the present investigation, we have used immunocytochemical and immunoblotting techniques to study the expression of CSPGs in the thalamus of the rat during postnatal development. Moreover, with double-labeling techniques, we have investigated the distribution of perineuronal nets in adult thalamus in relation to the expression of the calcium-binding proteins that identify functionally distinct populations of neurons (Celio 1990; Arai et al. 1994; Winsky et al. 1992; Lizier et al. 1997).

Materials and methods

Animals

Postnatal rats (Wistar; Charles River, Calco, Italy), ranging from the day of birth (defined as postnatal day 0, P0) to the end of the third postnatal week, and adult rats weighing about 250 g were used. The University of Milan approved the care and handling of animals in accordance with all NIH guidelines.

Antibodies

The following mouse monoclonal antibodies (MAbs) were used: MAb CS-56 (IgM, Sigma, St. Louis, Mo.), which recognizes the 6-sulfated and, with lower affinity, the 4-sulfated forms of an as yet poorly characterized epitope present in the interior of native chondroitin sulfate (Avnur and Geiger 1984; Sorrel et al. 1993); MAbs 1-B-5 and 2-B-6 (IgG, ICN Pharmaceuticals, Costa Mesa, Calif.), which recognize oligosaccharide stubs resulting from the digestion of CSPGs with chondroitinase ABC and containing a terminal unsaturated hexuronic acid adjacent either to unsulfated N-acetylgalactosamine (1-B-5) or to 4-sulfated N-acetylgalactosamine (2-B-6; Caterson et al. 1985). For double-labeling experiments, MAb 1-B-5 was used in combination with either polyclonal anti-calretinin or polyclonal anti-parvalbumin antibodies (SWant, Bellinzona, Switzerland).

Electrophoresis and Western blot analysis

Adult and 4-day-old rats were anesthetized by intraperitoneal injection of chloral hydrate (4%, 1 ml/100 g body weight) and transcardially perfused with ice-cold 50 mM TRIS-HCl buffer, pH 6.5, containing 0.15 M NaCl, 2 mM EDTA, 100 µM N-ethylmaleimide, 500 µM phenylmethylsulfonyl fluoride. A thick brain slice including the thalamus was homogenized in a glass-Teflon homogenizer in five volumes of ice-cold perfusion buffer to which 1 µg/ml pepstatin and leupeptin had been added. After removal of the low speed pellet (800 *g* for 10 min), the supernatant was centrifuged at 100,000 *g* for 30 min, and the resulting supernatant was collected.

A few aliquots of the homogenate were dialyzed against 0.1 M TRIS-HCl, pH 7.2, containing 0.1 M Na acetate and digested with chondroitinase ABC (Sigma, 5 mU/100 µg protein) in the presence of proteinase inhibitors for 2 h at 37°C.

After separation by SDS-polyacrylamide gel electrophoresis (SDS-PAGE; 5% separating gels), proteins were transferred to nitrocellulose. The blots, with or without previous digestion with chondroitinase ABC, were sequentially probed with primary antibodies and the appropriate horseradish-peroxidase-labeled secondary antibody. Immunoreactivity was detected by using the BM chemiluminescence Western blotting kit (Boehringer, Mannheim, Germany) according to the manufacturer's instructions. Chemiluminescent bands were recorded on Kodak X-Omat AR films.

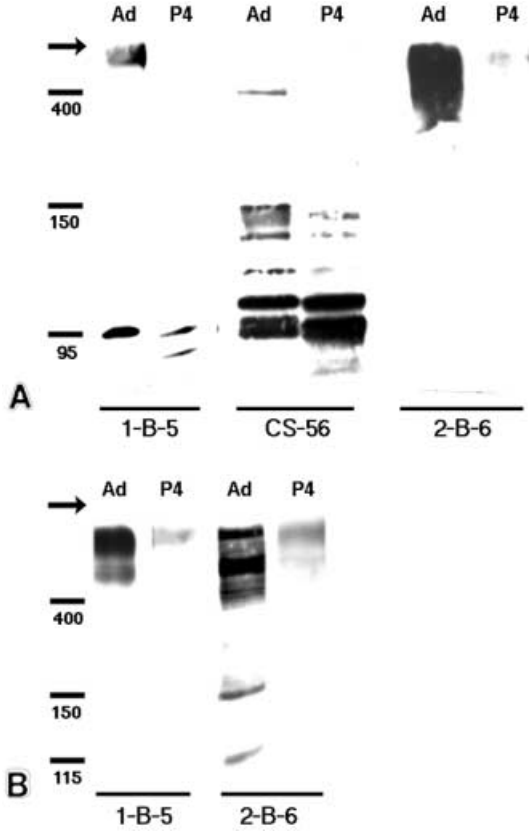

Fig. 1 Immunoblot analysis of homogenates from P4 (*P4*) and adult (*Ad*) brain not subjected (**A**) or subjected (**B**) to digestion with chondroitinase ABC before SDS-PAGE. The amount of protein loaded per lane was 100 µg (*arrows* gel top). Molecular weights are in kDa

Light and confocal microscopy

At least three animals were used at each selected age (P0, P2, P5, P7, P9, P11, P15, P18, P20, adult). The animals, under deep anesthesia, were perfused transcardially with 1% paraformaldehyde in 0.1 M phosphate buffer (PB), pH 7.2, followed by a mixture of 4% paraformaldehyde and 0.5% glutaraldehyde in the same buffer. The brains were then dissected out, postfixed in 4% paraformaldehyde for 12 h, and embedded in paraffin or serially cut in coronal sections (50 µm) on a Vibratome throughout the rostrocaudal extent of the thalamus. Selected paraffin or vibratome sections were incubated in primary antibody. Antigen-antibody reaction was revealed by the standard ABC-peroxidase method (Hsu et al. 1981) with the Vectastain ABC kit (Vector Laboratories, Burlingame, Calif.) and diaminobenzidine tetrahydrochloride (DAB) as a chromogen. Prior to immunoreaction with 1-B-5 and 2-B-6 MAbs, sections were subjected to enzymatic digestion with 0.2 U/ml chondroitinase ABC in 0.1 M TRIS-HCl, pH 7.2, containing 0.1 M Na acetate and 20 µg/ml bovine serum albumin (BSA; 75 min at 37°C). In other experiments, sections were digested with 100 U/ml *Streptomyces* hyaluronidase (Sigma) in 0.05 M acetate buffer, pH 5 (3 h at 37°C), prior to incubation with MAb 1-B-5. The incubation media for enzyme digestion always contained a cocktail of protease inhibitors.

Control sections were submitted to the same immunocytochemical staining sequence, except that the primary antibody was omitted or replaced with equivalent concentrations of unrelated IgM or IgG of the same subclass.

For double-labeling experiments, sections were incubated with a mixture of MAb 1-B-5 and anti-parvalbumin or anti-calretinin serum**.** Sections were subsequently incubated with a mixture of

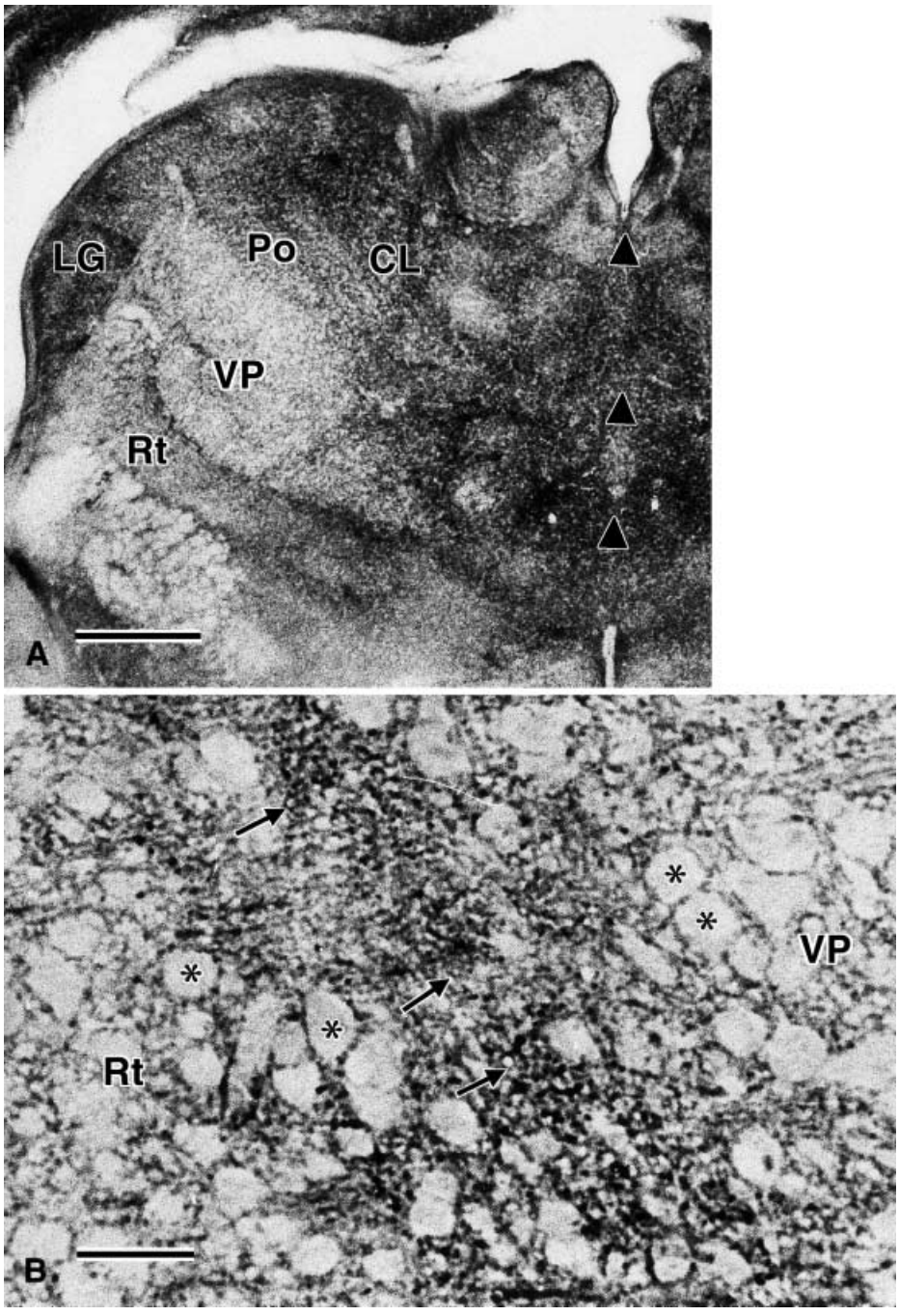

Fig. 2A, B Light micrographs of coronal vibratome sections of rat thalamus showing the distribution of CS-56 immunoreactivity during the first week of life. ABC-DAB method. **A** Intermediate part of the thalamus at P1. **B** Detail of the distribution of CS-56 immunoreactivity in Rt and ventroposterior nucleus at P5. *Asterisks* and *arrows* indicate, respectively, neuronal cell bodies and transversely sectioned nerve fibers outlined by immunoreactivity (*CL* central lateral nucleus, *LG* lateral geniculate nucleus, *Po* thalamic posterior complex, *Rt* reticular nucleus, *VP* ventroposterior nucleus). *Bars* **A** 500 µm, **B** 50 µm

the appropriate fluorescein-isothiocyanate-conjugated or lissamine-rhodamine-conjugated secondary antibodies (Jackson Immunoresearch, West Grove, Pa.). Double-labeled vibratome sections were examined under a TCS NT confocal laser scan microscope (Leica Lasertechnik, Heidelberg, Germany).

Immunoelectron microscopy

Brain coronal sections, fixed as for light microscopy immunocytochemistry, were permeabilized by a mild ethanol treatment (10%, 25%, and 10%; 5 min each) or with 0.2% saponin in PB containing 1% BSA (3 changes; 10 min each). Sections were subsequently immunolabeled with MAb CS-56 or 1-B-5 according to the ABC method, postfixed with 1% osmium tetroxide, and flat-embedded in Epon-Spurr. Ultrathin sections of the regions of interest were cut on a Reichert ultramicrotome and examined (unstained or counterstained with lead citrate only) with a Zeiss 902 electron microscope. Electron-spectroscopic imaging procedures were routinely employed to improve contrast.

Results

Western blot analysis

Both 1-B-5 and 2-B-6 (Fig. 1A) MAbs recognized high molecular weight components (over 400 kDa) only in adult brain homogenates. An additional band of approxi-

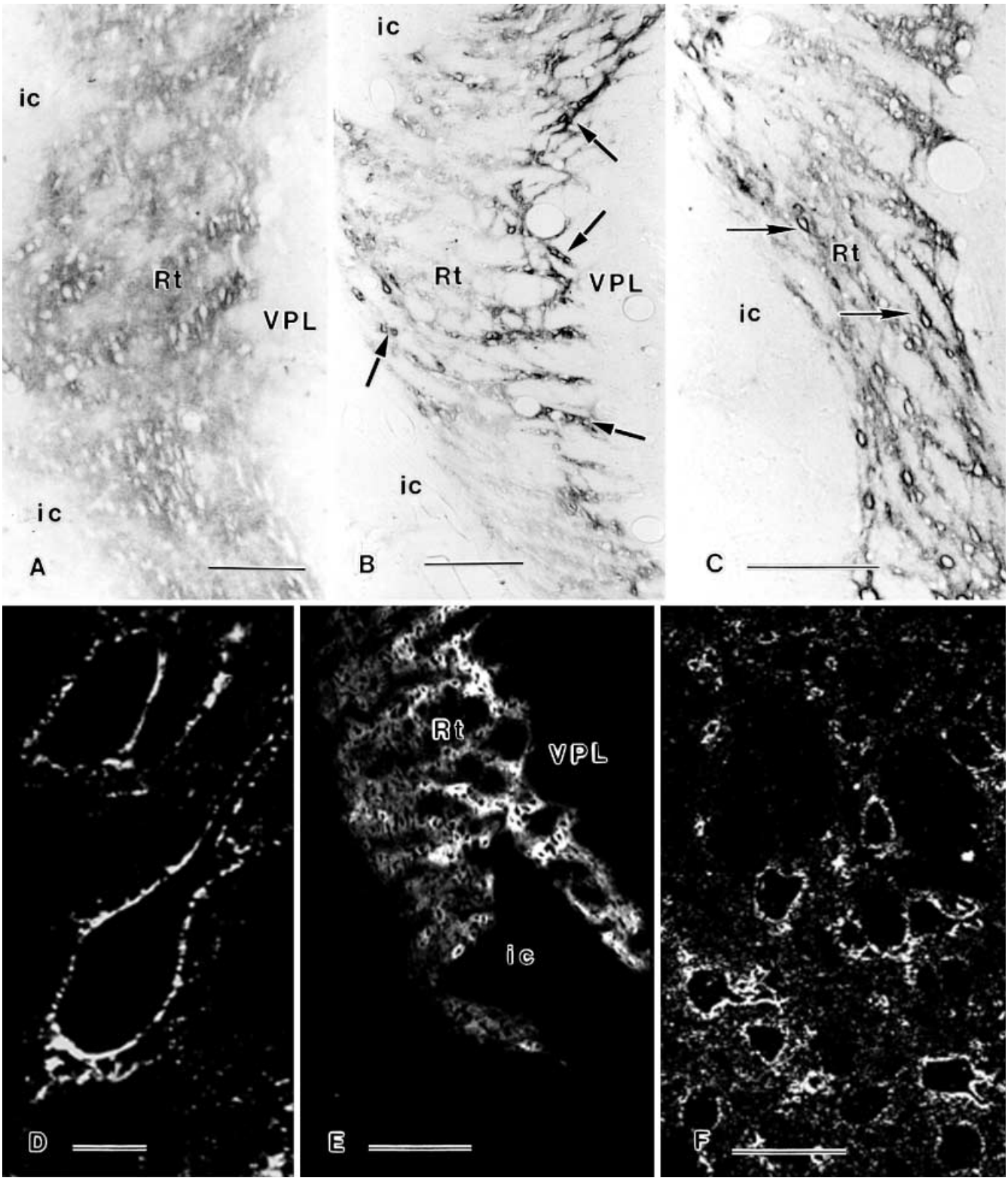

Fig. 3 Light micrographs of coronal paraffin sections of the thalamus immunostained with MAb 1-B-5. **A–C** ABC-DAB method. **D–F** Immunofluorescence. The micrographs show the distribution of immunoreactivity in Rt at P15 (**A**) and in adult thalamus (**B–F**). Thicker perineuronal nets (*arrows*) are recognizable along the medial and lateral aspects (**B**) and in the ventromedial corner (**C**) of the intermediate part of Rt. **D** Detail of perineuronal nets in Rt. **E** posterior sector of Rt. **F** Distribution of the immunoreactivity in the medial part of ventroposterior nucleus. *ic* Internal capsule, *Rt* reticular nucleus, *VPL* lateral part of ventroposterior nucleus. *Bars* **A–C** 200 µm, **D** 10 µm, **F** 50 µm

mately 95 kDa was recognized by MAb 1-B-5 in both P4 and adult brain.

Digestion of brain extracts with chondroitinase ABC prior to electrophoresis increased the mobility of the core proteins recognized by 1-B-5 and 2-B-6 antibodies (Fig. 1B). The intensities of all bands were higher in the adult than in P4 samples. Both antibodies identified at least two bands with molecular weight over 400 kDa and with similar electrophoretic mobility, whereas MAb 2-B-6 recognized additional bands of approximately 400, 150, and 120 kDa.

The CS-56 antibody revealed several components of molecular weights between 95 and 150 kDa, and only in adult brain fraction, an additional component of about 400 kDa (Fig. 1A). Two major bands of approximately 100 kDa appeared to be more intense in P4 brain than in adult brain fractions. No immunoreactive bands were recognized by this antibody in blots submitted to preliminary digestion with chondroitinase ABC.

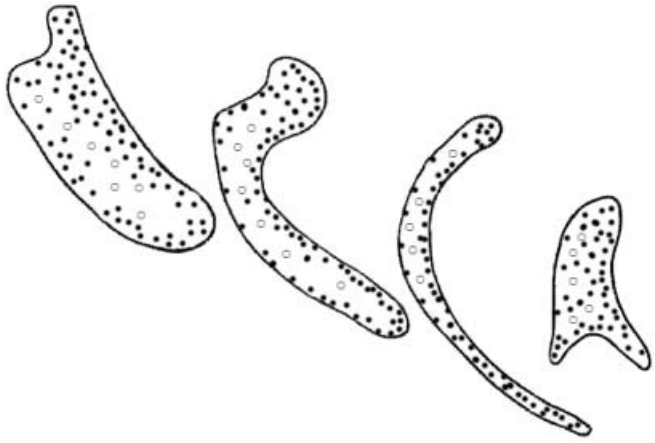

Fig. 4 Schematic representation of the distribution of perineuronal nets at different rostrocaudal levels (from *left* to *right*) of adult Rt (*black* and *open dots* indicate, respectively, the distribution of thick and thin perineuronal nets)

Immunocytochemistry

The pattern of labeling obtained with all antibodies was highly reproducible in animals of comparable age. No immunostaining was found in control sections in which the primary antibody was replaced with unrelated IgM or IgG.

In the first postnatal week, MAbs CS-56 and 1-B-5 gave a similar labeling pattern consisting of finely granular material forming a delicate meshwork in the neuropil of all thalamic nuclei (Fig. 2A), whereas cell bodies were always unstained (Fig. 2B). The intensity of labeling varied among the different thalamic nuclei whose boundaries were frequently outlined by the accumulation of immunoreactive material (Fig. 2A). The level of immunostaining was maximum in the laterodorsal, lateroposterior, and lateral geniculate nuclei and in most midline nuclei, and minimum in the ventral posterolateral and ventroposterior nucleus (Fig. 2A) and in the anteroventral and anteromedial nuclei.

During the second postnatal week, immunoreactivity decreased progressively. On P12, CS-56 immunostaining was detectable only in the neuropil of Rt and of a few midline nuclei, and, after P15, it was no longer recognizable. Labeling for MAb 1-B-5 declined in most thalamic nuclei but remained intense in the neuropil of Rt and of most midline nuclei.

During the third postnatal week, except for a light and diffuse positivity in the neuropil of midline nuclei, immunoreactivity for MAb 1-B-5 was mainly concentrated in Rt, in which perineuronal staining became recognizable around a few neurons at about P15 (Fig. 3A). At the end of the third week, the labeling pattern of Rt attained the adult configuration (Figs. 3B–E), and intensely labeled perineuronal nets surrounded the perikarya and proximal dendrites of several neurons.

In adult thalamus, the distribution of perineuronal nets and their labeling intensity varied along the rostrocaudal axis of Rt (Fig. 4). The rostral and caudal (Fig. 3E) parts of Rt and the ventromedial corner in the intermediate sector of the nucleus (Fig. 3C) displayed strong staining of perineuronal nets and of the intervening neuropil. Moreover, the thickest and most intensely labeled perineuronal nets were concentrated along the medial and, to a lesser extent, lateral edges of the nucleus (Figs. 3B, E, 5A, C, E). Conversely, perineuronal nets were very thin or absent in the central part of the intermediate sector of Rt (Fig. 3B).

Outside Rt, a small cluster of thin perineuronal nets was consistently observed in the dorsal part of the central lateral nucleus. Sparse and less intensely labeled perineuronal nets were also detected in the ventroposterior (Fig. 3F) and posterior nuclei, whereas diffuse faint neuropilar immunoreactivity persisted in most midline nuclei.

The distribution of chondroitin 4-sulfate, identified by MAb 2-B-6, was notably different from that of the other antigens examined, since, only at the perinatal stage, thin meshworks of immunoreactive material were recognizable only in the neuropil of the lateroposterior nucleus and of the midline nuclei. With increasing age, even this positivity decreased to a very pale and diffuse background. With this antibody, perineuronal nets were never observed in the thalamus, although, in the same sections, they were intensely labeled throughout the cerebral cortex.

Pretreatment of sections with chondroitinase ABC before immunostaining with MAb CS-56 abolished immunoreactivity. Omission of chondroitinase ABC pretreatment abolished immunostaining with MAbs 1-B-5 and 2-B-6. Pretreatment of sections with *Streptomyces* hyaluronidase before immunostaining with MAb 1-B-5 produced an intense immunostaining of the neuropil of all thalamic nuclei only at the perinatal stage.

Double immunolabeling for perineuronal nets and calcium-binding proteins in adult thalamus

Since perineuronal nets are mainly concentrated in Rt, the study of their association with calcium-binding pro-

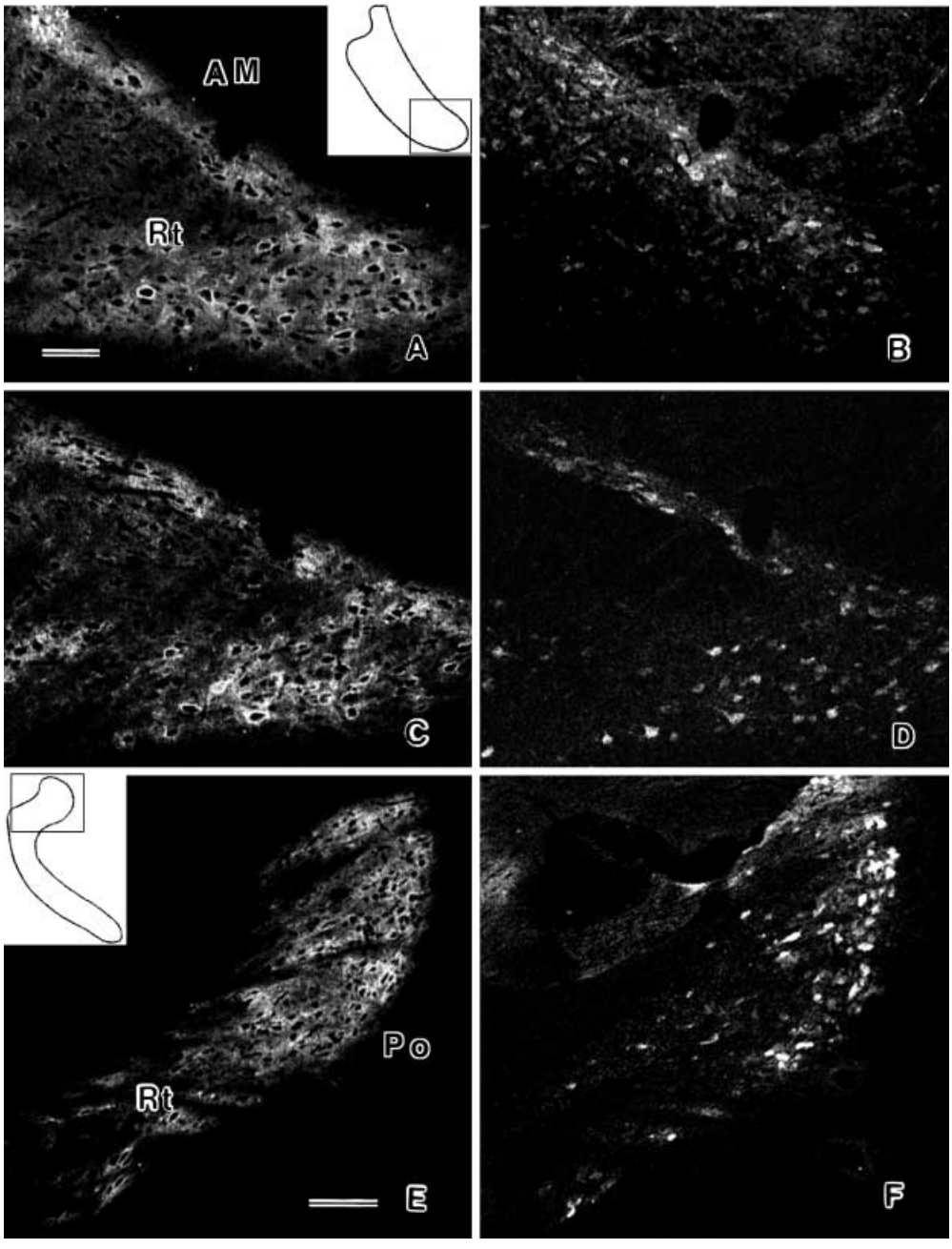

Fig. 5 Analysis by confocal microscope of vibratome sections of adult Rt double-labeled with MAb 1-B-5 (**A, C, E**) and with either anti-parvalbumin (**B**) or anti-calretinin (**D, F**) antibodies. *Insets* Position at which coronal sections were taken along the rostrocaudal axis of the nucleus. **A–D** Ventromedial corner of the anterior part of Rt. **E, F** Rostral pole of the intermediate sector of Rt. *AM* Anteromedial nucleus, *Po* thalamic posterior complex, *Rt* reticular nucleus. *Bars* 100 µm (**C** same magnification as **A**)

teins has been focused on this nucleus. Previous studies (Celio 1990; Arai et al. 1994; Winsky et al. 1992; Lizier et al. 1997) have shown that most neurons of Rt contain parvalbumin, whereas calretinin and calbindin have a more restricted distribution.

The results of our double-labeling experiments showed that the association between neuronal positivity for parvalbumin and perineuronal nets was extended, but not total. The most notable exceptions were represented by (1) the weak pericellular staining in the central part of the intermediate Rt (Fig. 3B) in which all neurons express parvalbumin (not shown); (2) the strong staining of both perineuronal nets and the intervening neuropil in the ventral border of the rostral medial corner, an area almost devoid of parvalbulmin-positive neurons (Fig. 5A, B).

In general, the most intense labeling of perineuronal nets and neuropil matched the distribution of calretinin-positive neurons, which were especially concentrated in the rostral (Fig. 5C, D) and caudal sectors of Rt, in the dorsal cap of the intermediate part of the nucleus (Fig. 5E, F), and along the medial and lateral edges. However, even within these areas, not all calretinin-positive neurons were surrounded by pericellular staining.

At high magnification, the distribution of immunoreactivity for MAb 1-B-5 around cell bodies and proximal dendrites of neurons positive for either parvalbumin or calretinin appeared to be similar (Fig. 6A–D). Moreover, in many

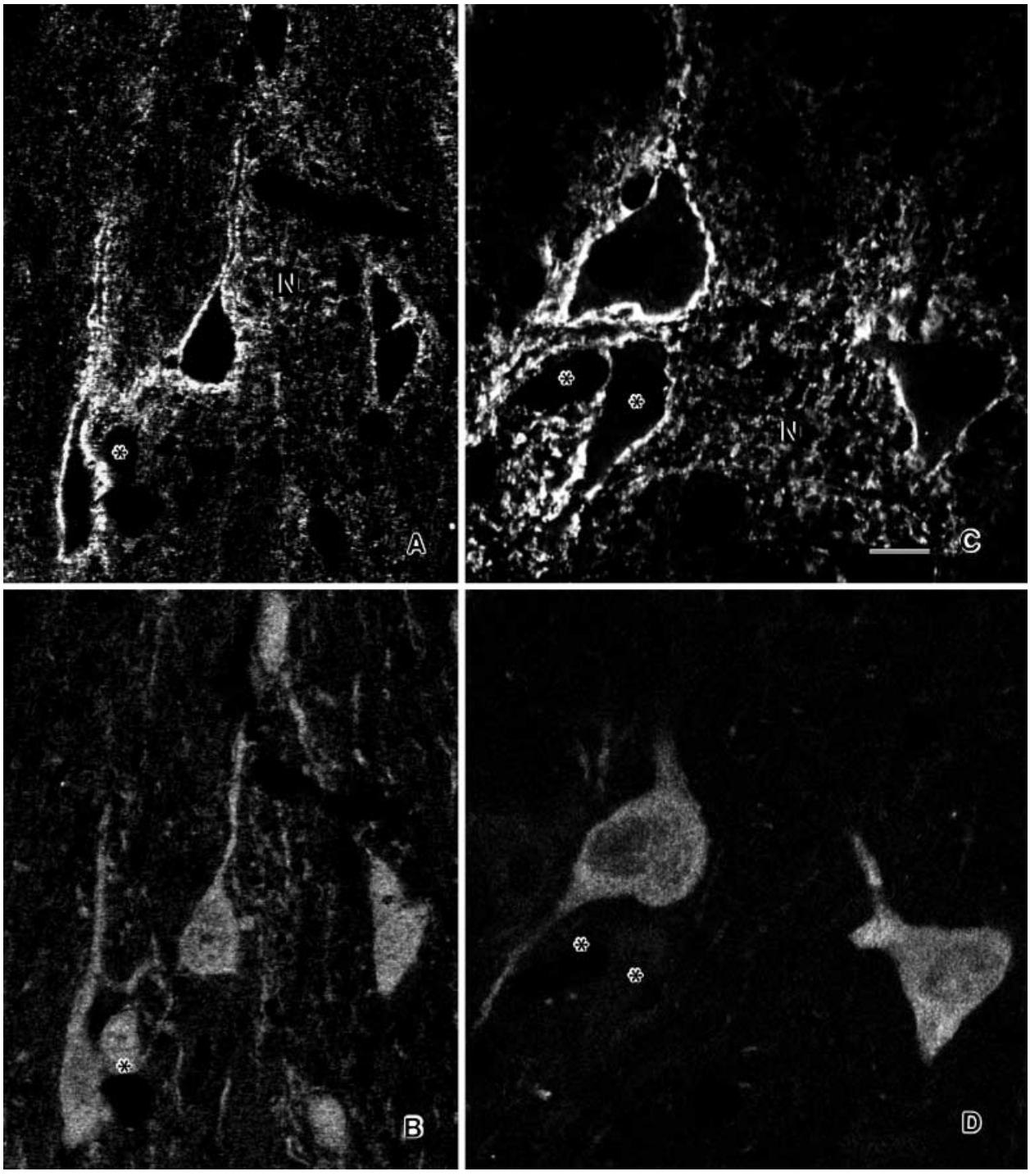

Fig. 6 Confocal micrographs showing, at higher magnification, perineuronal nets in adult Rt double-labeled with MAb 1-B-5 (**A, C**) and with either anti-parvalbumin (**B**) or anti-calretinin (**D**) antibodies. **A, B** Neurons located in proximity of the medial edge of the intermediate sector of Rt (*asterisk* parvalbumin-positive neuron lacking perineuronal net). **C, D** Dorsal cap of the intermediate sector of Rt. Both calretinin-positive and negative (*asterisk*s) neurons are enwrapped by perineuronal nets (*N* neuropil). *Bars* 10 μm

neuropil regions, 1-B-5 immunoreactivity associated with dendrite surfaces produced dense reticulate staining (Fig. 6A, C). Outside Rt, a correlation between perineuronal nets and calretinin was found in neurons of the dorsal part of central lateral nucleus and in the midline nuclei.

Immunoelectron microscopy

At early postnatal stages, the immunoreactivity for MAbs CS-56 and 1-B-5 was concentrated around the

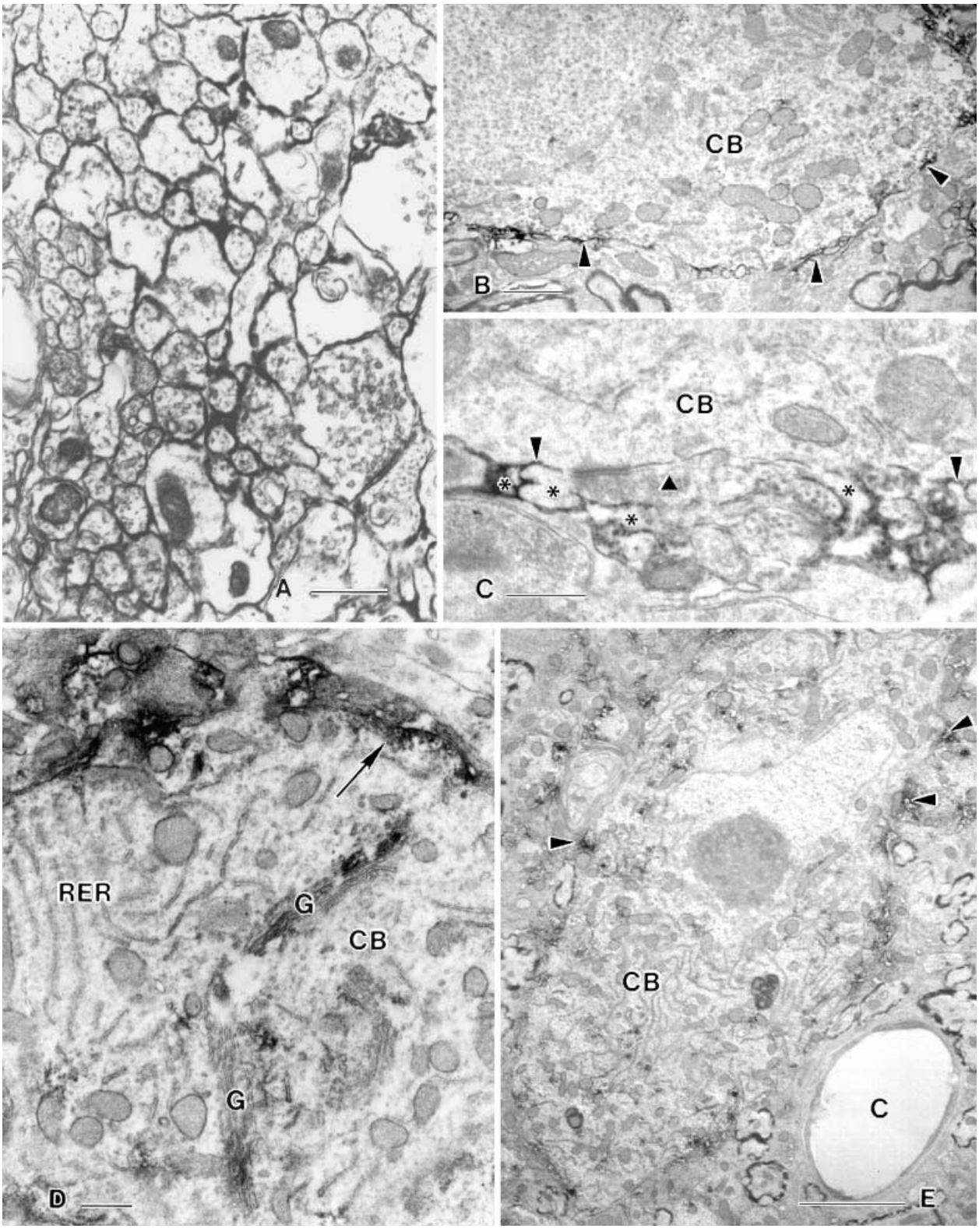

Fig. 7 **A** Electron micrograph of Rt neuropil at P5 showing nerve processes outlined by immunoreactivity for MAb CS-56. **B, C** Electron micrographs of neuronal cell bodies (*CB*) in adult Rt labeled with MAb 1-B-5 after mild ethanol permeabilization (*arrowheads* immunoreactivity outlining a cell body). In **C,** labeled astrocytic processes (*asterisks*) are adjacent to an unlabeled terminal making an asymmetric axosomatic synapse (*triangle*). **D, E** Electron micrographs of neuronal cell bodies (*CB*) in adult Rt (**D**) and in central lateral nucleus (**E**) labeled with MAb 1-B-5 after saponin permeabilization. Immunoreactivity is present around cell bodies (*arrowheads*), in Golgi complexes (*G*), and in small vesicles (*arrow*). *C* Capillary, *RER* rough endoplasmic reticulum. Counterstaining with lead citrate. *Bars* **A, C** 0.5 µm, **B, D** 1 µm, **E** 3 µm

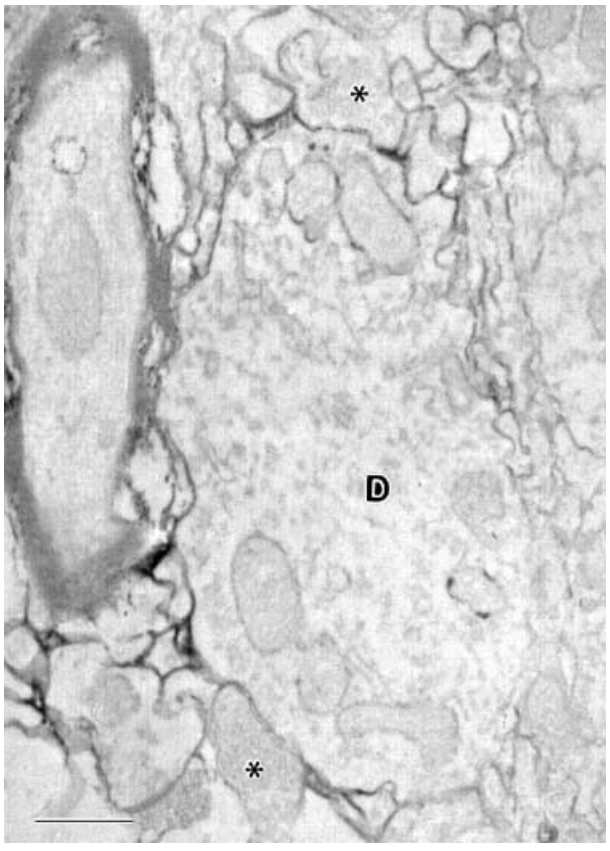

Fig. 8 Electron micrograph of adult Rt neuropil showing a dendrite (*D*) outlined by immunoreactivity for MAb 1-B-5 and contacted by two terminals (*asterisks*) making symmetric axodendritic synapses. Counterstaining with lead citrate. *Bar* 0.5 μm

plasma membranes of nerve fibers, terminals (Fig. 7A), and perikarya. In adult Rt, perineuronal labeling for MAb 1-B-5 outlined perikaryal and dendritic plasma membranes, being interrupted by unlabeled synaptic contacts (Figs. 7B, C, 8). MAb 1-B-5 labeling was found inside and around astrocytic processes close to neuronal cell bodies (Fig. 7C). Perivascular astrocytes were always unlabeled (Fig. 7E). When tissues were permeabilized with saponin, immunoreactivity was also detected in the Golgi apparatus and in small vesicles clustered near the inner aspect of neuronal plasma membranes (Fig. 7D), but not in astrocytic cell bodies. MAb 1-B-5 immunoreactivity, although less intense and sparser, showed a similar pattern of distribution in the dorsal part of central lateral nucleus (Fig. 6E) and in the ventroposterior nucleus.

Discussion

The distribution of CSPGs in the central nervous system has so far been investigated by immunocytochemistry with two types of antibodies. The first type recognizes the protein core and provides a selective identification of one molecular species. Conversely, antibodies of the second type, directed against the carbohydrate moieties, should have a broader specificity for several CSPGs bearing similar GAGs. Indeed, antibodies of the second type have been frequently used as general markers of CSPGs (Miller et al. 1995; Hoffman-Kim et al. 1998). To address the question of the specificity of the antibodies (belonging to the second type) used in this investigation, we carried out Western blotting experiments on homogenates of whole brain at two representative ages (P4 and adult). The results show that MAbs CS-56, 1-B-5, and 2-B-6 identify mostly nonoverlapping molecular species of CSPGs. These findings are in line with previous observations (Sorrel et al. 1996) showing that GAG chains are not random polymers of disaccharides but consist of domains that, in different CSPGs, are assembled in specific combinations. MAb CS-56 recognizes several components, most of which are expressed both at P4 and in adult brain and have apparent molecular weights between 95 kDa and 150 kDa. MAbs 1-B-5 and 2-B-6 recognize higher-molecular-weight components that are predominantly expressed in adult brain and that seem to overlap partially, thus indicating that the same CSPGs may exist in different sulfation forms. The absence of immunoreactivity for MAb CS-56 in the high-molecular-weight components recognized by 1-B-5 and 2-B-6 antibodies indicates that the GAG moieties of these molecules lack, or have undetectable levels, of the 4/6-sulfated epitopes recognized by the former antibody. These findings agree with previous observations (Sorrel et al. 1996) indicating that MAb CS-56 cannot be considered a generic marker for CSPGs.

The immunocytochemical analysis of the thalamus has shown that the distribution of CS-56 and 1-B-5 epitopes during postnatal development is similar to that previously described for the cerebral cortex (Miller et al. 1995). With both antibodies, immunoreactivity is intense after birth and decreases progressively until it disappears (MAb CS-56) or becomes restricted to the perineuronal nets of distinct neuronal populations (MAb 1-B-5). The presence of components immunoreactive for MAb CS-56 observed in adult brain with Western blotting might be accounted for by the persistence of immunoreactivity in brain regions not considered in this study. Moreover, the masking of CS-56 epitopes may occur during tissue maturation and contribute to the decline of the immunoreactivity observed in histologic sections.

With respect to MAb 1-B-5, the intense positivity displayed only by the neonatal thalamus after digestion with bacterial hyaluronidase suggests that hyaluronan contributes to the immunoreactivity observed at this stage. This interpretation agrees with (1) the results of Western blotting experiments showing that CSPG(s) recognized by MAb 1-B-5 in neonatal brain are scanty, and (2) previous observations indicating that hyaluronan is abundant in brain at early developmental stages (Bignami et al. 1993). Moreover, it is known that MAb 1-B-5 also recognizes d-unsaturated disaccharides of hyaluronan (Caterson et al. 1985) generated either by bacterial hyaluronidase, an enzyme that hydrolyses only

hyaluronan (Derby and Pintar 1978), or by enzymes with a broader specificity, such as chondroitinase ABC.

On the basis of the results obtained with MAb 2-B-6, it appears that CSPGs with 4-sulfated initial GAGs contribute only in a limited fashion to the extracellular matrix of the immature thalamus and, at variance with the cerebral cortex, are no longer detectable in the adult organ. The latter finding indicates that regional differences exist in the regulation of the enzymes of the GAG biosynthetic pathway, probably in relation to specific functional requirements.

Overall, our observations confirm that CSPGs and hyaluronan have a widespread distribution in the brain during the first postnatal week. In particular, these molecules could fill the extracellular spaces, which are wider in neonatal than in adult brain (Lehmenkühler et al. 1993), thereby regulating the osmotic and swelling pressure of the tissue. Moreover, the highly hydrated environment provided by GAGs and their capacity to bind morphogenetic factors (Celio and Blümcke 1994) may favor the processes of reorganization, remodeling, and maturation still active in the thalamus during the first two postnatal weeks (Frassoni et al. 1995; De Biasi et al. 1996). The postnatal appearance of perineuronal nets at the onset of the third week of life has been previously observed with lectin histochemistry (Köppe et al. 1997) and corresponds to the time of acquisition of the mature neuronal phenotype (Spreafico et al. 1994; De Biasi et al. 1996, 1997).

Immunocytochemical and Western blotting results indicate that the CSPG(s) recognized by MAb 1-B-5 in adult thalamus, viz., the high-molecular-weight forms that exhibit the prevalent expression in mature brain and whose synthesis probably involves neurons, share features with CSPGs that contain Cat antigens (Hockfield and McKay 1983; Hockfield et al. 1990; Fryer et al. 1992; Lander et al. 1998) and that are related to aggrecan (Fryer et al. 1992).

Our immunocytochemical data extend previous observations (Bertolotto et al. 1991, 1996) on the presence of 1-B-5-positive perineuronal nets in adult rat thalamus. In particular, we have observed that differences exist in the labeling intensity of perineuronal nets throughout the rostrocaudal extension of Rt. This nucleus belongs to the ventral thalamus and consists of a population of projecting gamma-aminobutyric-acid-ergic cells (De Biasi et al. 1986) that provide an inhibitory innervation to all nuclei of the dorsal thalamus (Steriade et al. 1997). The vast majority of Rt neurons express parvalbumin and, to a lesser extent, calretinin and calbindin (Celio 1990; Winsky et al. 1992; Arai et al. 1994; Lizier et al. 1997). The present data demonstrate that the strongest labeling of the perineuronal nets and of the intervening neuropil matches the distribution of calretinin-positive neurons. This association, however, does not correspond to functionally homogeneous sectors of Rt. Indeed, the most intense labeling of perineuronal nets has been detected in the rostral pole of Rt, which is connected to limbic functions, and, more caudally, in the visual and acustic sectors. Moreover, a strong pericellular staining is associated with neurons distributed along the medial edge of the whole nucleus. These marginal neurons, although belonging to functionally different sectors, share a number of features, such as their morphology (Spreafico et al. 1991), their preferential expression of calretinin (Lizier et al. 1997; present study), and their distinctive expression of neurofilament subunits and adhesive molecules (A. Amadeo, personal communication), and may represent a subpopulation with distinct, although as yet unknown, functional properties. Interestingly, in the rat, neurons of the inner tier of the somatosensitive, visual, and acustic sectors of the Rt nucleus are connected with higher order thalamic nuclei and with secondary cortical areas (Guillery et al. 1998). The correlation of perineuronal nets with calbindin has not been studied in the present investigation. However, previous studies have shown (Arai et al. 1994) that, in Rt, calbindin-positive neurons are few and are concentrated in the central part of the ventromedial corner, a region nearly devoid of pericellular nets.

The cellular origin of CSPGs varies according to molecular species, since they can be of either neuronal or glial origin or both (Yamaguchi 2000). Our ultrastructural observations, showing the presence of 1-B-5 immunoreactivity in astrocytic processes and in the Golgi complex of neurons, should be interpreted cautiously and are not sufficient to support an involvement of both cell types in the biosynthesis of 1-B-5-immunoreactive molecules.

With regard to the function of perineuronal nets, attempts to correlate their presence with specific physiological properties of neurons have not to date given unequivocal results (for reviews, see Celio and Blümcke 1994; Celio et al. 1998), even if a growing body of evidence seems to indicate that they may be involved in the regulation of the ionic composition in the pericellular environment (Spicer et al. 1996; Härtig et al. 1999). It has been also proposed that perineuronal nets, consisting of tertiary complex of CSPGs, hyaluronan and tenascin-R, may play a role in the regulation of synaptic plasticity and stabilization (for reviews, see Celio et al. 1998; Yamaguchi 2000).

In conclusion, the results of this investigation confirm recent findings on the architectural and neurochemical complexity of Rt and the existence of complicate relationships between perineuronal nets and neuronal physiology. Therefore, further work is needed to correlate the neurochemical and synaptic features of neurons enwrapped by perineuronal nets with the composition of the pericellular matrix, whose microchemical complexity and heterogeneity probably imply diversified functions in different regions of the central nervous system.

References

Aquino DA, Margolis RU, Margolis RK (1984) Immunocytochemical localization of a chondroitin sulfate proteoglycan in nervous tissue. II. Studies in developing brain. J Cell Biol 99:1130–1139

Arai R, Jacobowitz DM, Deura S (1994) Distribution of calretinin, calbindin-D28 k, and parvalbumin in the rat thalamus. Brain Res Bull 33:595–614

Avnur Z, Geiger B (1984) Immunocytochemical localization of native chondroitin sulfate in tissues and cultured cells using specific monoclonal antibody. Cell 38:811–822

Bertolotto A, Rocca G, Schiffer D (1990) Chondroitin 4-sulfate proteoglycan forms an extracellular network in human and rat central nervous system. J Neurol Sci 100:113–123

Bertolotto A, Rocca G, Canavese G, Migheli A, Schiffer D (1991) Chondroitin sulfate proteoglycan surrounds a subset of human and rat CNS neurons. J Neurosci Res 29:225–234

Bertolotto A, Manzardo E, Guglielmone R (1996) Immunohistochemical mapping of perineuronal nets containing chondroitin unsulfate proteoglycan in the rat central nervous system. Cell Tissue Res 283:283–295

Bignami A, Hosley M, Dahl D (1993) Hyaluronic acid and hyaluronic acid-binding proteins in brain extracellular matrix. Anat Embryol 188:419–433

Brückner G, Härtig W, Kacza J, Seeger J, Welt K, Brauer K (1996) Extracellular matrix organization in various regions of rat brain grey matter. J Neurocytol 25:333–346

Caterson B, Christner JE, Baker JR, Couchman JR (1985) Production and characterization of monoclonal antibodies directed against connective tissue proteoglycans. Fed Proc 44:386–393

Celio MR (1990) Calbindin D-28 k and parvalbumin in the rat nervous system. Neuroscience 35:375–475

Celio MR, Blümcke I (1994) Perineuronal nets – a specialized form of extracellular matrix in the adult nervous system. Brain Res Rev 19:128–145

Celio MR, Spreafico R, De Biasi S, Vitellaro-Zuccarello L (1998) Perineuronal nets: past and present. Trends Neurosci 21:510–515

Crabtree JW, Kind PC (1993) Monoclonal antibody Cat-301 selectively identifies a subset of nuclei in the cat's somatosensory thalamus. J Neurocytol 22:903–812

De Biasi S, Frassoni C, Spreafico R (1986) GABA immunoreactivity in the thalamic reticular nucleus of the rat: a light and electron microscopical study. Brain Res 399:143–147

De Biasi S, Amadeo A, Arcelli P, Frassoni C, Meroni A, Spreafico R (1996) Ultrastructural characterization of the postnatal development of the thalamic ventrobasal and reticular nuclei in the rat. Anat Embryol 193:343–353

De Biasi S, Amadeo A, Arcelli P, Frassoni C, Spreafico R (1997) Postnatal development of GABA-immunoreactive terminals in the reticular and ventrobasal nuclei of the rat thalamus: a light and electron microscopic study. Neuroscience 76:503–516

Derby MA, Pintar JE (1978) The histochemical specificity of *Streptomyces* hyaluronidase and chondroitinase ABC. Histochem J 10:529–547

Fernaud-Espinosa I, Nieto-Sampedro M, Bovolenta P (1996) Developmental distribution of glycosaminoglycans in embryonic rat brain: relationship to axonal tract formation. J Neurobiol 30:410–424

Flaccus A, Janetzko A, Tekotte H, Margolis RK, Margolis RU (1991) Immunocytochemical localization of chondroitin and chondroitin 4-sulfates and 6-sulfates in developing rat cerebellum. J Neurochem 56:1608–1615

Frassoni C, Arcelli P, Regondi MC, Selvaggio M, De Biasi S, Spreafico R (1995) Branching pattern of corticothalamic projections from the somatosensory cortex during postnatal development in the rat. Dev Brain Res 90:111–121

Fryer HJL, Kelly GM, Molinaro L, Hockfield S (1992) The high molecular weight Cat-301 chondroitin sulfate proteoglycan from brain is related to the large aggregating proteoglycan from cartilage, aggrecan. J Biol Chem 267:9874–9883

Gray D, Gutierrez C, Cusick CG (1999) Neurochemical organization of inferior pulvinar complex in squirrel monkeys and macaques revealed by acetylcholinesterase histochemistry, calbindin and Cat-301 immunostaining, and *Wisteria floribunda* agglutinin binding. J Comp Neurol 409:452–468

Guillery RW, Feig SL, Lozsádi DA (1998) Paying attention to the thalamic reticular nucleus. Trends Neurosci 21:28–32

Härtig W, Derouiche A, Welt K, Brauer K, Grosche J, Mäder M, Reichenbach A, Brückner G (1999) Cortical neurons immunoreactive for potassium channel Kv3.1b subunit are predominantly surrounded by perineuronal nets presumed as a buffering system for cations. Brain Res 842:15–29

Hartmann U, Maurer P (2001) Proteoglycans in the nervous system – the quest for functional roles in vivo. Matrix Biol 20:23–35

Hendry SH, Jones EG, Hockfield S, McKay RDG (1988) Neuronal populations stained with the monoclonal antibody Cat-301 in the mammalian cerebral cortex and thalamus. J Neurosci 8:518–542

Herndon ME, Lander AD (1990) A diverse set of developmentally regulated proteoglycans is expressed in the rat central nervous system. Neuron 4:949–961

Hockfield S, McKay RDG (1983) A surface antigen expressed by a subset of neurons in the vertebrate central nervous system. Proc Natl Acad Sci USA 80:5758–5761

Hockfield S, McKay RDG, Hendry SH, Jones EG (1983) A surface antigen that identifies ocular dominance columns in the visual cortex and laminar features of the lateral geniculate nucleus. Cold Spring Harbor Symp Quant Biol 48:877–889

Hockfield S, Kalb RG, Zaremba S, Fryer HJL (1990) Expression of neural proteoglycans correlates with the acquisition of mature neuronal properties in the mammalian brain. Cold Spring Harbor Symp Quant Biol 55:505–514

Hoffman-Kim D, Lander AD, Jhaveri S (1998) Patterns of chondroitin sulfate immunoreactivity in the developing tectum reflects regional differences in glycosaminoglycan biosynthesis. J Neurosci 18:5881–5890

Hsu SM, Raine L, Fanger H (1981) Use of avidin-biotin-peroxidase complex (ABC) in immunoperoxidase techniques: a comparison between ABC and unlabeled antibody (PAP) procedures. J Histochem Cytochem 29:557–580

Köppe G, Brückner G, Brauer K, Härtig W, Bigl V (1997) Developmental patterns of proteoglycan-containing extracellular matrix in perineuronal nets and neuropil of the postnatal rat brain. Cell Tissue Res 288:33–41

Lander C, Zhang H, Hockfield S (1998) Neurons produce a neuronal cell surface-associated chondroitin sulfate proteoglycan. J Comp Neurol 18:174–183

Lehmenkühler A, Syková E, Svoboda J, Zilles K, Nicholson C (1993) Extracellular space parameters in the rat neocortex and subcortical white matter during postnatal development determined by diffusion analysis. Neuroscience 55:339–351

Letourneau PC, Condic ML, Snow DM (1994) Interactions of developing neurons with the extracellular matrix. J Neurosci 14:915–928

Lizier C, Spreafico R, Battaglia G (1997) Calretinin in the thalamic reticular nucleus of the rat: distribution and relationship with ipsilateral and contralateral efferents. J Comp Neurol 377:217–233

Maeda N, Hamanata H, Oohira A, Noda M (1995) Purification, characterization and developmental expression of a brain-specific chondroitin sulfate proteoglycan, 6B4 proteoglycan/phosphacan. Neuroscience 67:23–35

Margolis RK, Margolis RU (1994) Nervous tissue proteoglycans. In: Jollès P (ed) Nervous tissue proteoglycans. Birkhäuser, Basel, pp 145–177

Matsui F, Nishizuka M, Oohira A (1999) Proteoglycans in perineuronal nets. Acta Histochem Cytochem 32:141–147

Miller B, Sheppard AM, Bicknese AR, Pearlman AL (1995) Chondroitin sulfate proteoglycans in the developing cerebral cortex: the distribution of neurocan distinguishes forming afferent and efferent axonal pathways. J Comp Neurol 355: 615–628

Oohira A, Katoh-Semba R, Watanabe E, Matsui F (1994) Brain development and multiple molecular species of proteoglycan. Neurosci Res 20:195–207

Pimenta AF, Strick PL, Levitt P (2001) Novel proteoglycan epitope expressed in functionally discrete pattern in primate cortical and subcortical regions. J Comp Neurol 430:369–388

Preuss TM, Gray D, Cusick CG (1998) Subdivisions of the motor and somatosensory thalamus of primates revealed with *Wisteria floribunda* agglutinin histochemistry. Somatosens Mot Res 15:211–219

Rauch U, Gao P, Janetzko A, Flaccus A, Hildenberg L, Tekotte H, Margolis RK, Margolis RU (1991) Isolation and characterization of developmentally regulated chondroitin sulfate and chondroitin/keratan sulfate proteoglycans of brain identified with monoclonal antibodies. J Biol Chem 266:14785–14801

Seeger G, Brauer K, Härtig W, Brückner G (1994) Mapping of perineuronal nets in the rat brain stained by colloidal iron hydroxide histochemistry and lectin cytochemistry. Neuroscience 58:371–388

Sorrel JM, Carrino DA, Caplan AI (1993) Structural domains in chondroitin sulfate identified by anti-chondroitin sulfate monoclonal antibodies. Immunosequencing of chondroitin sulfates. Matrix 13:351–361

Sorrel JM, Carrino DA, Caplan AI (1996) Regulated expression of chondroitin sulfates at sites of epithelial-mesenchimal interaction: spatio-temporal patterning identified with anti-chondroitin sulfate monoclonal antibodies. Int J Dev Neurosci 14:233–248

Spicer SS, Naegele JR, Schulte BA (1996) Differentiation of glycoconjugates localized to sensory terminals and selected sites in brain. J Comp Neurol 365:217–231

Spreafico R, Battaglia G, Frassoni C (1991) The reticular thalamic nucleus (RTN) of the rat: cytoarchitectural, Golgi, immunocytochemical, and horseradish peroxidase study. J Comp Neurol 304:478–490

Spreafico R, Frassoni P., Arcelli P, Battaglia G, Wenthold RJ, De Biasi S (1994) Distribution of AMPA selective glutamate receptors in the thalamus of adult rats and during postnatal development. A light and ultrastructural immunocytochemical study. Brain Res Dev Brain Res 82:231–244

Steriade M, Jones EG, McCormic DA (1997) Thalamus, vol I. Organization and function. Elsevier, Amsterdam

Sur M, Frost DO, Hockfield S (1988) Expression of a surface-associated antigen on Y-cells in the lateral geniculate nucleus is regulated by visual experience. J Neurosci 8:874–882

Winsky L, Montpied P, Arai R, Martin BM, Jacobowitz DM (1992) Calretinin distribution in the thalamus of the rat: immunohistochemical and in situ hybridization histochemical analyses. Neuroscience 50:181–196

Yamaguchi Y (2000) Chondroitin sulfate proteoglycans in the nervous system. In: Iozzo RV (ed) Proteoglycans. Dekker, New York Basel, pp 379–402